

Catalytic Study of Methanol-to-Propylene Conversion over Nano-Sized HZSM-5

Jianwen Li, Hongfang Ma, Weixin Qian, Haitao Zhang, Weiyong Ying

Abstract—Methanol-to-propylene conversion was carried out in a continuous-flow fixed-bed reactor over nano-sized HZSM-5 zeolites. The HZSM-5 catalysts were synthesized with different Si/Al ratio and silicon sources, and treated with NaOH. The structural property, morphology, and acidity of catalysts were measured by XRD, N₂ adsorption, FE-SEM, TEM, and NH₃-TPD. The results indicate that the increment of Si/Al ratio decreased the acidity of catalysts and then improved propylene selectivity, while silicon sources had slight impact on the acidity but affected the product distribution. The desilication after alkali treatment could increase intracrystalline mesopores and enhance propylene selectivity.

Keywords—Alkali treatment, HZSM-5, methanol-to-propylene, synthesis condition.

I. INTRODUCTION

PROPYLENE, as one of most important raw materials in modern chemical industry, is mainly produced by steam cracking and fluid catalytic cracking [1]. However, these oil-based traditional technologies cannot meet the increasing demand of propylene [2]. Thus, nonpetroleum routes to produce propylene are more considered in academia and industry. Methanol-to-propylene (MTP) conversion has attracted much attention, because propylene selectivity is relatively high and methanol can be easily obtained via synthesis gas from coal, natural gas and biomass [3]–[5].

Zeolite catalysts have been broadly utilized in industrial processes, owing to outstanding properties [6], [7]. For the conversion of methanol-to-hydrocarbons, various zeolites have been tested as catalysts. Compared with other zeolites, HZSM-5 has been considered as an effective catalyst to produce propylene in MTP [5], [8], [9]. Nevertheless, HZSM-5 catalyst still needs to be modified in order to improve its catalytic performance. One of crucial problems for HZSM-5 catalyst is deactivation caused by coking during reaction [5], [10], [11].

Previous literatures have reported that synthesis conditions could affect the catalytic performance of HZSM-5 zeolite catalysts in the conversion of MTP [11], [12]. Meanwhile, alkali treatment can also improve the catalytic performance of

HZSM-5 catalysts through generating mesopores. Herein, the study investigated the effect of Si/Al ratio, silicon sources and alkali treatment on HZSM-5, and physiochemical properties of catalysts were characterized by XRD, N₂ adsorption, FE-SEM, TEM and NH₃-TPD.

II. EXPERIMENTAL

A. Catalyst Preparation

Tetrapropylammonium hydroxide (TPAOH, 2 M aqueous solution) and tetraethylorthosilicate (TEOS) were mixed and stirred at 70 °C for 10 h. After that, the aqueous solution which contained aluminum nitrate and NaOH was added to the mixture. Then, the mother gel obtained was crystallized at 170 °C for 20 h with stirring. After crystallization, the Na-ZSM-5 was collected by centrifugation, washed to neutral with deionized water, dried at 110 °C for 16 h, and then calcined at 550 °C for 10 h with a heating rate of 3 °C·min⁻¹. The molar ratio of mother gel was 1SiO₂: (1/x)Al₂O₃: 0.15TPAOH: 0.02NaO₂: 20H₂O (x=100, 200). The obtained Na-ZSM-5 zeolites were named as T-Z-x.

NaOH and NaAlO₂ were dissolved in the solution of TPAOH, and then silica sol was dropped into the solution. 10 wt.% silicalite-1 seed was added into the mixture. Then, the mother gel obtained was crystallized at 170 °C for 24 h with stirring. After crystallization, the zeolite was collected by centrifugation, washed to neutral with deionized water, dried at 110 °C for 16 h, and then calcined at 550 °C for 10 h with a heating rate of 3 °C·min⁻¹. The molar ratio of mother gel was 1SiO₂: (1/100)Al₂O₃: 0.15TPAOH: 0.02NaO₂: 20H₂O (x=100, 200). The obtained Na-ZSM-5 zeolites were named as S-Z-100.

T-Z-100 was treated with a 0.2 M NaOH solution (33 mL solution per gram catalyst material) for 30 min at 65 °C, followed by cooling in an ice bath to stop the desilication, washing with water and centrifuging three times, and then drying at 110 °C for 12 h. The obtained sample was named as T-Z-100-AT.

Four-fold Na⁺/NH₄⁺ ion-exchange with 1 M NH₄Cl was performed at 80 °C for 2 h on T-Z-x, T-Z-100-AT and S-Z-100. The resulting samples were filtrated, washed, and dried at 110 °C and finally calcined at 550 °C for 6 h. Then, the H-form zeolites (T-HZ-x, T-HZ-100-AT and S-HZ-100) were obtained.

B. Catalyst Characterization

Wide-angle XRD patterns were taken with a Rigaku Multiflex diffractometer equipped with Cu K α radiation (40 kV, 40 mA).

N₂ adsorption was performed on a Micrometrics ASAP 2020 instrument at -196 °C. Prior to N₂ adsorption, the catalysts were

Jianwen Li, Hongfang Ma, Weixin Qian, and Haitao Zhang are with Engineering Research Center of Large Scale Reactor Engineering and Technology, Ministry of Education, State Key Laboratory of Chemical Engineering, East China University of Science and Technology, Shanghai 200237, China.

Weiyong Ying is with Engineering Research Center of Large Scale Reactor Engineering and Technology, Ministry of Education, State Key Laboratory of Chemical Engineering, East China University of Science and Technology, Shanghai 200237, China (phone: 86-21-64252192; fax: 86-21-64252192; e-mail: wying@ecust.edu.cn).

outgassed under vacuum at 350 °C for 4 h.

Field-emission scanning electron microscopic (FE-SEM) images of the samples were obtained on Nova NanoSEM 45, microscope operating at 1-30 kV. The samples for FE-SEM were coated by platinum on QUORUM Q150RS before observation. Transmission electron microscope (TEM) images of the samples were acquired with a JEOL JEM-1400 instrument.

NH₃-TPD spectra were measured on a Micrometrics AutoChem II 2920 instrument. Samples were first flushed with He gas flow at 600 °C for 1 h in a U shaped quartz tube, and then cooled to 100 °C. Ammonia was adsorbed at 100 °C for 0.5 h. After flushing with He gas flow to remove physically absorbed ammonia, NH₃-TPD was started from 100 to 600 °C at a heating rate of 10 °C·min⁻¹. The desorbed ammonia was detected on the thermal conductivity detector (TCD).

C. Catalytic Test

The catalytic performance of catalysts was measured in a fixed-bed flow reactor with 10 mm inner diameter for MTP reaction. Prior to the reaction, the catalyst powder was pressed, crushed and sieved to 40-60 mesh particles. The catalyst was heated to 550 °C and kept for 2 h under N₂ gas flow. Then, the temperature was decreased to 450 °C. Pure methanol was injected by a pump into the reactor with methanol weight hourly space velocity of 5 h⁻¹. The catalyst loading amount was 0.5 g, and the reaction was carried out at 450 °C and atmospheric pressure. The gaseous products were analyzed via an GC6890C gas chromatograph equipped with a 50 m HP-PLOT Al₂O₃ capillary column and a flame ionization detector (FID). The liquid oil phase was collected and analyzed by Agilent 7890A (FID, HP-5), and the liquid aqueous phase, including mainly water, methanol, and dimethyl ether (DME), was analyzed with Agilent GC 6820 (TCD, Plot Q). DME was considered to be unconverted reactant in the calculation of conversion and selectivity.

III. RESULTS AND DISCUSSION

A. Textural Properties

The XRD patterns of HZSM-5 zeolite catalysts are shown in Fig. 1. It can be noted that all catalysts, including parent zeolites and base leached zeolites, exhibited obvious representative peaks corresponding to the MFI structure. This indicates that the framework structure of HZSM-5 was maintained in the process of alkali treatment. However, the XRD intensity of alkali treated HZSM-5 was much lower than the parent HZSM-5, implying the decreased crystallinity.

The textural properties of the catalysts were investigated by N₂ adsorption. As listed in Table I, the surface areas and pore volumes in T-HZ-100, T-HZ-200, and S-HZ-100 had no distinct difference. It can be concluded that Si/Al ratio and silicon sources exert little impact on the surface area and pore volume of HZSM-5 zeolites. However, T-HZ-100-AT had much higher surface area and pore volume than T-HZ-100, and the increase mainly derived from the enhancement of mesopore surface area and pore volume. These results indicate that

mesopores were generated on HZSM-5 after base leaching. Fig. 2 shows the pore size distribution of catalysts. The untreated HZSM-5 catalysts had obvious pore distribution peaks at 2 nm. For T-HZ-100-AT, besides the peak at 2 nm, it had also a broad peak in the range from 3 to 15 nm. Meanwhile, the intensity of peak at 2 nm on T-HZ-100-AT decreased compared with T-HZ-100. These results also imply the formation of mesopores.

TABLE I
SUMMARY OF SURFACE AREAS AND TOTAL PORE VOLUMES OF CATALYSTS

| Catalyst | S_{BET} (m ² ·g ⁻¹) | S_{meso} (m ² ·g ⁻¹) | V_{p} (cm ³ ·g ⁻¹) | V_{meso} (cm ³ ·g ⁻¹) |
|-------------|---|--|--|---|
| T-HZ-100 | 339 | 120 | 0.27 | 0.16 |
| T-HZ-200 | 347 | 122 | 0.30 | 0.20 |
| S-HZ-100 | 360 | 124 | 0.27 | 0.15 |
| T-HZ-100-AT | 413 | 228 | 0.54 | 0.45 |

S_{BET} : BET surface area, V_{p} : total pore volume

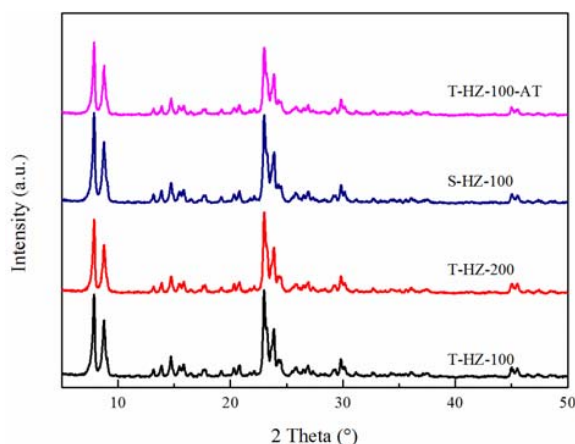


Fig. 1 XRD patterns of catalysts

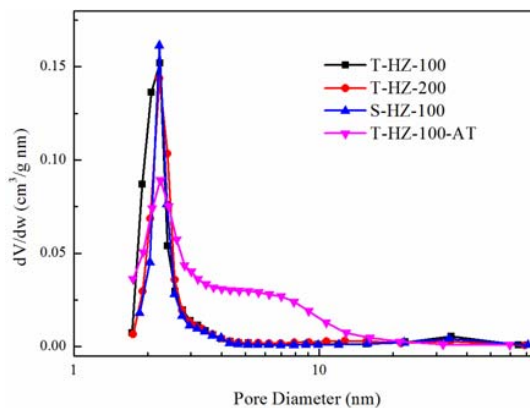


Fig. 2 BJH pore size distribution of catalysts

B. FE-SEM and TEM

Fig. 3 shows the FE-SEM images of HZSM-5 zeolite catalysts. It can be noted that all catalysts have an average particle size of 100-200 nm. Si/Al ratio did not affect the crystal appearance. The zeolite synthesized from silica sol was slightly larger than those synthesized from TEOS. Compared with T-HZ-100, T-HZ-100-AT owned rougher surface, which might

be caused by the alkali treatment. The interior structure of alkali treated zeolite was illustrated in Fig. 4. The TEM image of T-HZ-100-AT shows that intracrystalline mesopores formed in the zeolite, which is in line with the results of N_2 adsorption.

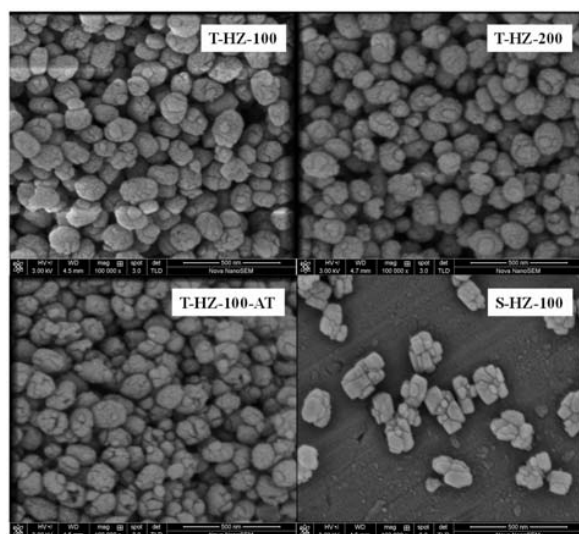


Fig. 3 FE-SEM images of catalysts

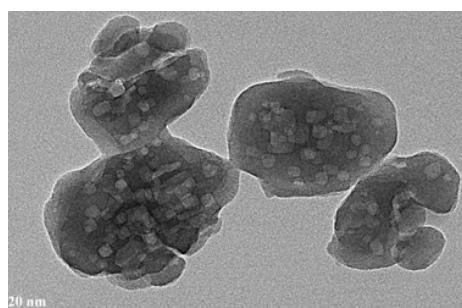


Fig. 4 TEM image of T-HZ-100-AT

C. Temperature Programmed Desorption of Ammonia

NH_3 -TPD was used to measure the amount and strength of acid sites on HZSM-5. Fig. 5 shows the NH_3 -TPD profiles of catalysts in the temperature range of 100 to 600 °C. T-HZ-100 showed a typical NH_3 -TPD spectrum with two desorption peaks at about 203 °C and 398 °C, clearly suggesting the existence of corresponding weak and strong acid sites, respectively. As Si/Al ratio increased, the amount of weak and strong acid sites both decreased. Compared with T-HZ-100, S-HZ-100 owned similar concentration of weak and strong acid sites, indicating that the silicon source played little role in the acidity of HZSM-5 zeolite. After alkali treatment, the amount of weak acid sites significantly increased, while that of strong weak sites showed little change. This indicates that the alkali treatment mainly generated new weak acid sites.

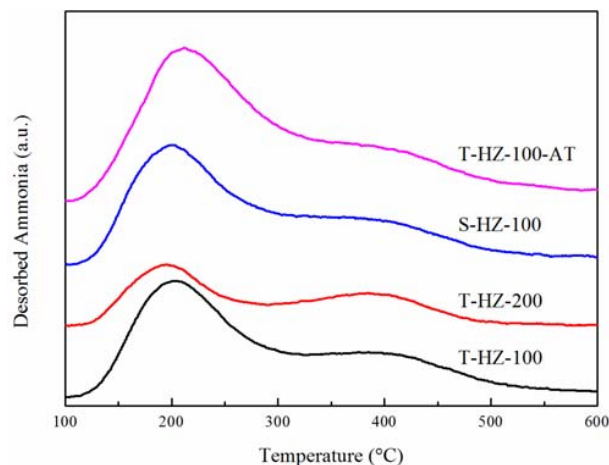


Fig. 5 NH_3 -TPD profiles of catalysts

D. Catalytic Performance of Catalysts in MTP

The conversion of methanol and the selectivities of products and in MTP reaction are listed in Table II. T-HZ-100 exhibited relatively low propylene selectivity and high C_{3-6} alkanes selectivity. As Si/Al increased, the propylene selectivity increased and C_{3-6} alkanes selectivity decreased. This could be explained by the reason that the increment of Si/Al ratio reduced the acidity, and then inhibited the hydrogen transfer reaction, decreasing the light alkane selectivity [11]. However, butene selectivity and pentene selectivity also increased on T-HZ-200 due to the decrement of acidity. When silica sol was used as silicon source, the synthesized S-HZ-100 also had the highest propylene selectivity and low C_{3-6} alkanes selectivity. Liang et al. [12] proposed that the aromatic-based cycle was preferential over HZSM-5 synthesized from TEOS with framework aluminum enriched in the channel intersections, whereas the alkene-based route was superior over HZSM-5 synthesized from silica sol with framework aluminum concentrated in the sinusoidal and straight channels. Therefore, S-HZ-100 owned the highest propylene selectivity. Propylene selectivity also increased on T-HZ-100-AT. Generated mesopores enhanced diffusivity of alkali treated zeolites, which could inhibit the secondary reactions of propylene [5], [10].

IV. CONCLUSION

HZSM-5 zeolites with different Si/Al ratios and silicon sources were prepared for MTP, and the synthesized HZSM-5 were treated with alkali solution. BET results and morphology images show that mesopores formed in zeolite after alkali treatment. NH_3 -TPD spectra indicate that the increment of Si/Al ratio reduced the acidity and alkali treatment increased the amount of acid sites, especially weak acid sites. The increment of Si/Al ratio and alkali treatment both improve propylene selectivity, but the HZSM-5 synthesized from silica sol owned highest propylene selectivity.

TABLE II
CATALYTIC PERFORMANCE OF CATALYSTS

| Catalyst | Conversion (%) | Selectivity (%) | | | | | | |
|-------------|----------------|------------------|-------------------------------|-------------------------------|-------------------------------|--------------------------------|------------------|--------|
| | | C ₁₋₂ | C ₂ H ₄ | C ₃ H ₆ | C ₄ H ₈ | C ₅ H ₁₀ | C ₃₋₆ | Others |
| T-HZ-100 | 100 | 2.05 | 11.81 | 16.63 | 8.82 | 2.05 | 43.10 | 15.54 |
| T-HZ-200 | 100 | 1.01 | 8.14 | 25.36 | 14.43 | 3.80 | 33.59 | 13.67 |
| S-HZ-100 | 100 | 1.94 | 12.46 | 26.40 | 9.98 | 3.08 | 35.59 | 10.55 |
| T-HZ-100-AT | 100 | 0.81 | 10.22 | 22.65 | 13.32 | 3.68 | 38.27 | 11.05 |

All the data were obtained at 2 h of time on stream

REFERENCES

- [1] A. Corma, F. Melo, L. Sauvanaud, F. Ortega, "Light cracked naphtha processing: Controlling chemistry for maximum propylene production," *Catal. Today*, Vol. 107, pp. 699-706, 2005.
- [2] X. Zhu, S. Liu, Y. Song, L. Xu, "Catalytic cracking of C4 alkenes to propene and ethene: Influences of zeolites pore structures and Si/Al₂ ratios," *Appl. Catal. A Gen.*, Vol. 288, pp. 134-142, 2005.
- [3] J. Liu, C. Zhang, Z. Shen, W. Hua, Y. Tang, W. Shen, Y. Yue, H. Xu, "Methanol to propylene: Effect of phosphorus on a high silica HZSM-5 catalyst," *Catal. Commun.*, Vol. 10, pp. 1506-1509, 2009.
- [4] U. V. Mentzel, K. T. Højholt, M. S. Holm, R. Fehrmann, P. Beato, "Conversion of methanol to hydrocarbons over conventional and mesoporous H-ZSM-5 and H-Ga-MFI: Major differences in deactivation behavior," *Appl. Catal. A Gen.*, Vol. 417-418, pp. 290-297, 2012.
- [5] L. Zhang, Y. Song, G. Li, Q. Zhang, S. Zhang, J. Xu, F. Deng, Y. Gong, "F-assisted synthesis of a hierarchical ZSM-5 zeolite for methanol to propylene reaction: a b-oriented thinner dimensional morphology," *RSC Adv.*, Vol. 5, pp. 61354-61363, 2015.
- [6] B. Kaur, R. Srivastava, B. Satpati, "Highly efficient CeO₂ decorated nano-ZSM-5 catalyst for electrochemical oxidation of methanol," *ACS Catal.*, Vol. 6, pp. 2654-2663, 2016.
- [7] S. Mitchell, M. Boltz, J. Liu, J. Perez-Ramirez, "Engineering of ZSM-5 zeolite crystals for enhanced lifetime in the production of light olefins via 2-methyl-2-butene cracking," *Catal. Sci. Technol.*, Vol. 7, pp. 64-74, 2017.
- [8] F. Yaripour, Z. Shariatnia, S. Sahebdehfar, A. Irandoukht, "Effect of boron incorporation on the structure, products selectivities and lifetime of H-ZSM-5 nanocatalyst designed for application in methanol-to-olefins (MTO) reaction," *Microporous Mesoporous Mater.*, Vol. 203, pp. 41-53, 2015.
- [9] H. Chen, Y. Wang, F. Meng, H. Li, S. Wang, C. Sun, S. Wang, X. Wang, "Conversion of methanol to propylene over nano-sized ZSM-5 zeolite aggregates synthesized by a modified seed-induced method with CTAB," *RSC Adv.*, Vol. 6, pp. 76642-76651, 2016.
- [10] C. Mei, P. Wen, Z. Liu, H. Liu, Y. Wang, W. Yang, Z. Xie, W. Hua, Z. Gao, "Selective production of propylene from methanol: Mesoporosity development in high silica HZSM-5," *J. Catal.*, Vol. 258, pp. 243-249, 2008.
- [11] Y. Kim, J.-C. Kim, C. Jo, T.-W. Kim, C.-U. Kim, S.-Y. Jeong, H.-J. Chae, "Structural and physicochemical effects of MFI zeolite nanosheets for the selective synthesis of propylene from methanol," *Microporous Mesoporous Mater.*, Vol. 222, pp. 1-8, 2016.
- [12] T. Liang, J. Chen, Z. Qin, J. Li, P. Wang, S. Wang, G. Wang, M. Dong, W. Fan, J. Wang, "Conversion of methanol to olefins over H-ZSM-5 zeolite: reaction pathway is related to the framework aluminum siting," *ACS Catal.*, Vol. 6, pp. 7311-7325, 2016.